Soft Matter

PAPER

View Article Online
View Journal | View Issue

Cite this: *Soft Matter*, 2016, 12, 1176

Temperature responsive behavior of polymer brush/polyelectrolyte multilayer composites†

Samantha Micciulla,[a] Olaf Soltwedel,[b] Oliver Löhmann[a] and Regine von Klitzing*[a]

Received 6th September 2015,
Accepted 14th November 2015

DOI: 10.1039/c5sm02256h

www.rsc.org/softmatter

The complex interaction of polyelectrolyte multilayers (PEMs) physisorbed onto end-grafted polymer brushes with focus on the temperature-responsive behavior of the system is addressed in this work. The investigated brush/multilayer composite consists of a poly(styrene sulfonate)/poly(diallyldimethylammonium chloride) (PSS/PDADMAC) multilayer deposited onto the poly(*N*-isopropylacrylamide-*b*-dimethylaminoethyl methacrylate) P(NIPAM-*b*-DMAEMA) brush. Ellipsometry and neutron reflectometry were used to monitor the brush collapse with the thickness decrease as a function of temperature and the change in the monomer distribution perpendicular to the substrate at temperatures below, across and above the phase transition, respectively. It was found that the adsorption of PEMs onto polymer brushes had a hydrophobization effect on PDMAEMA, inducing the shift of its phase transition to lower temperatures, but without suppressing its temperature-responsiveness. Moreover, the diffusion of the free polyelectrolyte chains inside the charged brush was proved by comparing the neutron scattering length density profile of pure and the corresponding PEM-capped brushes, eased by the enhanced contrast between hydrogenated brushes and deuterated PSS chains. The results presented herein demonstrate the possibility of combining a temperature-responsive brush with polyelectrolyte multilayers without quenching the responsive behavior, even though significant interpolyelectrolyte interactions are present. This is of importance for the design of multicompartment coatings, where the brush can be used as a reservoir for the controlled release of substances and the multilayer on the top as a membrane to control the diffusion in/out by applying different stimuli.

Introduction

The research area of responsive coatings accounts for a huge variety of materials, which are characterized by the capability of changing their structural properties according to the applied external stimuli.[1–3] A large number of responsive coatings consist of tethered polymer chains grown from solid substrates. Such systems are known as polymer brushes and can be prepared with variable grafting density, chain length, chemical composition and geometry.[1,4–6] The important advantages of polymer brushes are the mechanical stability, due to the covalent bonding to the substrate, and the high swelling ratio, which causes a significant thickness change upon switching between swollen and collapsed state in good and bad solvents, respectively. This makes them particularly interesting for controlled release,[7] tunable assembly of coated nanoparticles,[8] responsive nanoactuators[9,10] or for antifouling surfaces.[11,12]

More recently, complex systems produced by embedding surfactants,[13,14] gels[15,16] or nanoparticles[17–20] into polymer brushes have been studied, from which multiresponsive coatings with enlarged applicability as stimuli-responsive systems can be designed.

Among them, there are some examples of polyelectrolyte (PE) chains adsorbed onto charged polymer brushes. Rühe and coworkers[21,22] studied the adsorption efficiency of free PE chains onto oppositely charged PE brushes depending on parameters like chain length, pH and ionic strength for different combinations of strong and weak polyelectrolytes. Besides introducing the use of polymer brushes as alternative substrates to the classical metal or metal oxide surfaces (*e.g.* gold or silicon) for PEM assembly, their findings highlighted the relevant influence of the charge density of the polyelectrolyte brush on the uptake of polyelectrolyte chains. Later, Laurent *et al.*[23] discussed the different topologies of quaternized PDMAEMA(PSS/PDADMAC) systems by using brush substrates with different grafting densities (pancake and brush-like regimes), onto which either patches or homogeneous PE layers were formed. The surface morphology was also the object of studies by Moya *et al.*,[24] who discussed the topography of different brush/multilayer combinations in relation to the nature of their interpolymer interactions (electrostatic and hydrogen bonding). Stable brush/PEM systems with inverse geometry, *i.e.* PEM as an initiator

[a] *Stranski-Laboratorium, Institut für Chemie, Technische Universität Berlin, Strasse des 17. Juni 124, D-10623 Berlin, Germany. E-mail: klitzing@chem.tu-berlin.de*
[b] *Max-Planck-Institute for Solid State Research, Outstation at MLZ, Lichtenbergstr. 1, 85747 Garching, Germany*

† Electronic supplementary information (ESI) available. See DOI: 10.1039/c5sm02256h

layer to graft responsive polymer brushes, have been reported by Laschewsky and coworkers,[25] but no specific information on the internal structure or mutual interpenetration was mentioned.

It is reasonable that besides structural effects, the combination of two interacting polymer compartments might alter or even suppress the responsive behavior of the constituent parts. Therefore the design of multicompartment responsive systems requires a deep investigation of mutual effects on the structure and responsive behavior arising from the assembly of different compartments.

To the best of our knowledge, systematic investigations on this important aspect are lacking. We addressed this fundamental question by choosing a block copolymer brush with temperature responsive properties, poly(*N*-isopropylacrylamide-*b*-dimethylaminoethyl methacrylate) P(NIPAM-*b*-DMAEMA), which was used as the substrate for the adsorption of the poly(styrene sulfonate)/poly(diallyldimethylammonium chloride) (PSS/PDADMAC)$_2$ multilayer. The choice of this block copolymer was motivated by the design of a neutral, temperature responsive part coupled with a charged block, which serves as a substrate for efficient PE adsorption. The charged nature of the PDMAEMA in Milli-Q water (pH $\sim$ 5.5; pK_a $\sim$ 7.5[26]) makes it a suitable candidate for this purpose; in addition, the pH and temperature responsiveness of this polymer[27,28] might enhance the control of system properties and its applicability as a smart coating material. The presence of PNIPAM ensures the temperature responsive behavior even in the case of strong complexation between the polyelectrolyte brush and free PE chains. The temperature induced brush collapse and the change in the polymer and solvent distribution upon phase transition were studied by optical methods. In particular, ellipsometry was used to study the mechanism of brush collapse and extract the transition temperature T_{tr} from the change in the thickness over a broad temperature range. Neutron reflectometry was used to deduce the structure of the two systems at three characteristic temperatures, below (15 °C), within (35 °C) and above (65 °C) the phase transition. Taking advantage of the enhanced contrast between hydrogenated brushes and deuterated PSS chains, it was possible to highlight the diffusion of the free chains inside the brush.

Materials and methods

Materials and sample preparation

Silicon wafers Si(100) (Siltronic AG, Munich, Germany) and polished silicon blocks of (7 × 3.5 × 1) cm^3 were used as substrates for the synthesis of brushes. *N*-Isopropylacrylamide (NIPAM) (98%, stabilized by methylhydroquinone) was purchased from TCI Tokyo Chemical Industry (Tokyo, Japan). Dimethylaminoethyl methacrylate, 2,2-bipyridyl, *N*,*N*,*N*′,*N*″,*N*″-pentamethyldiethylene-triamine (PMDETA), Cu(I)Cl, Cu(II)Cl$_2$, poly(styrene sulfonate) sodium salt (PSS, 70 000 g mol^{-1}, PDI = 2.5) and methanol were from Sigma Aldrich (Germany). The polyelectrolyte poly(diallyldimethylammonium chloride) (PDADMAC, 72 000 g mol^{-1}, PDI = 1.75) was synthesized by free radical polymerization[29] at the Fraunhofer Institute for Applied Polymer Research IAP (Potsdam, Germany). Deuterated poly(styrene sulfonate) (dPSS, 78 300 g mol^{-1}, PDI = <1.20) was from Polymer Standard Service (Mainz, Germany). Sodium chloride NaCl (purity >99.9%) from Merck (Darmstadt, Germany) was used to adjust the ionic strength of the polyelectrolyte solutions. All reagents were used as received without any further purification.

Polymer brushes were synthesized by the grafting-from method using Atom Transfer Radical Polymerization (ATRP). Prior to brush synthesis, the silicon substrates were modified by a 2-bromo-2-methyl-*N*-[3-(triethoxysilyl)-propyl]-propanamide (BTPAm) monolayer.[23] The polymerization times were chosen in order to obtain a similar thickness for all the brush systems (between 37 and 47 nm, Table 1). The synthesis of PNIPAM brushes was adopted from the procedure of Fujie *et al.*[30] In brief, 2.00 g of NIPAM were dissolved in 50 mL of methanol/water mixture (1 : 1 v/v), followed by the addition of 183 μL of PMDETA and 20 mg of CuCl. The polymerization was carried out for 6 min and terminated by adding a saturated solution of $CuCl_2$ in water/methanol. For the preparation of the block copolymer P(NIPAM-*b*-DMAEMA), the PNIPAM-modified substrates were transferred into a mixture of 33 mL of *N*,*N*-dimethylaminoethyl methacrylate (DMAEMA) 11.6 g of H_2O, 0.45 g of methanol, 2.00 g of bipyridyl and 0.40/0.04 g of CuCl/$CuCl_2$, according to the protocol reported by Bain *et al.*[31] The polymerization was run for 2 h, followed by sonication in methanol, rinsing in Milli-Q water and drying in a N_2 stream.

Polyelectrolyte solutions were prepared by dissolving the required amount of polyelectrolyte, PSS or PDADMAC, in 0.1 M NaCl solution to obtain the concentration of 0.01 (mono)mol L^{-1}. A layer-by-layer deposition method[32] was used to deposit PEMs onto the P(NIPAM-*b*-DMAEMA) brushes by alternately immersing the substrates in PSS and PDADMAC solutions for 10 min. The rinsing step was done in Milli-Q water and the deposition cycle was carried out twice. Finally the samples were dried in a nitrogen stream and stored in Petri dishes or plastic jars.

Table 1 Thickness and refractive index obtained from ellipsometric measurements under ambient conditions (21 °C, 30% r.h.) and in water (15 °C). In brackets the standard deviation values of the experimental values are reported. All the samples were prepared on individual silicon substrates. The volume ratio PNIPAM/PDMAEMA in the block copolymer was 1.65

	Air (21 °C, 30% r.h.)		Water (15 °C)		
Sample	n	d [nm]	n	d [nm]	ϕ_{sw} [%]
PNIPAM	1.472(4)	42.4(9)	1.393(5)	98.0(1)	57.0(9)
PDMAEMA	1.472(3)	47.7(4)	1.399(5)	118.7(1)	60.4(3)
P(NIPAM-*b*-DMAEMA)	1.525(2)	44.4(6)	1.399(5)	111.4(1)	60.0(7)
P(NIPAM-*b*-DMAEMA)(PSS/PDADMAC)$_2$	1.510(3)	93(3)	1.415(5)	212.2(2)	56.2(8)
PEI(PSS/PDADMAC)$_2$	1.54(4)	8.1(1)	1.46[35]	12(1)	33(6)

Methods

Ellipsometry. Ellipsometry is a non-destructive, optical technique based on the detection of the change in the polarized light upon reflection from a substrate. The changes in the amplitude and the phase of the reflected light are described by two parameters, ψ and Δ, which are related to the reflectivity properties of the sample by the fundamental equation of ellipsometry:

$$\tan\psi \cdot e^{i\Delta} = \frac{r_p}{r_s} \quad (1)$$

with r_p and r_s being the reflection coefficients of the components parallel and perpendicular to the reflection plane. The use of an appropriate layer model, which describes the measured system (substrate–film–medium), is necessary to obtain the optical properties (thickness d and refractive index n) from the experimental Δ and ψ, which describe the interaction between the polarized light and the sample. Detailed literature is available on the topic.[33,34]

The measured Δ and ψ were fitted with a three box model consisting of, from the bottom to the top, (i) silicon substrate (n = 3.88) as continuum 1, (ii) silicon oxide (n = 1.46, d = 1.5 nm), (iii) initiator BTPAm monolayer (n = 1.50,[23] d = 0.7 nm), (iv) polymer (n,d) and (v) water (n = 1.33) as continuum 2.

All the brush samples were prepared with a thickness between 40 and 50 nm as determined by ellipsometry under ambient conditions (21 °C, 30% r.h.). The volume ratio PNIPAM/PDMAEMA in the block copolymer was 1.65. From the measured thickness, the percentage of swelling water ϕ_{sw} was calculated according to the following equation:

$$\phi_{sw} = \frac{d_{sw}^{T} - d_{amb}}{d_{sw}^{T}} \quad (2)$$

where d_{sw}^{T} is the swollen thickness at temperature T and d_{amb} is the sample thickness measured under ambient conditions (21 °C, 30% r.h.). Experimental data and the calculated values of swelling water are reported in Table 1.

The change in thickness induced by the increase of temperature with respect to the initial swollen thickness was quantified by using the following relation:

$$\frac{d_{sw}^{T} - d_{sw}^{15\,°C}}{d_{sw}^{15\,°C}} \times 100 = \frac{\Delta d}{d_{sw}^{15\,°C}} \times 100[\%] \quad (3)$$

where $d_{sw}^{15\,°C}$ is the initial swollen brush thickness (15 °C) and d_{sw}^{T} is the swollen thickness at temperature $T > 15$ °C for the samples swollen in water. Eqn (3) gives negative values for Δd since d_{sw}^{T} is always smaller than $d_{sw}^{15\,°C}$.

Ellipsometric measurements were carried out using a Multiscope Null-Ellipsometer from Optrel GbR (Sinzing, Germany). The instrument is equipped with a red laser (λ = 632.8 nm) and a PCSA (polarizer–compensator–sample–analyzer) setup. Light guides drive the incident beam directly to the substrate/water interface to avoid the reflection at the liquid/air interface. Prior to measurement, the sample was soaked in a stainless steel cell filled with water at 15 °C for at least 30 min. A thermal cycle was applied by heating the solution by means of a copper plate underneath the sample holder. The temperature of the liquid environment was measured continuously with a precision of ±0.01 °C during the ellipsometric measurement by means of a temperature sensor immersed in the sample cell.

Neutron reflectometry. Neutron reflectometry (NR) exploits the reflection of a neutron beam as a function of momentum transfer Q. In the specular regime, the incident angle equals the reflected angle, therefore the technique is sensitive to the Q_z component only, from which it follows

$$Q_z = \frac{4\pi}{\lambda}\sin(\Theta) \quad (4)$$

where Θ is the angle of incidence and λ the neutron wavelength (0.43 nm). Neutron reflectivity measurements were carried out using the NREX reflectometer at the Heinz Maier-Leibnitz Zentrum in Garching (Munich, Germany). The samples were placed on a poly(tetrafluoroethylene) trough with stainless steel inlet and outlet tubes mounted in opposite corners to inject the liquid inside the cell. The silicon block was placed therein and it was sealed with a Viton O-ring. Detailed descriptions can be found in previous studies.[36,37] Heavy water, D_2O, was injected into the trough, and the samples were left equilibrating for at least 1 h prior to measurement.

The Motofit package[38] running in the Igor Pro environment (Wavemetrics) was used to fit the measured reflectivity curves, using a model to gain the corresponding SLD profiles. The model consisted of a set of two or three layers characterized by thickness d, scattering length density SLD and Gaussian roughness σ to mimic the realistic interfaces between the individual layers. The lowest possible number of boxes was used, from which reasonable fits could be obtained. The SLD profiles were optimized using a Levenberg–Marquardt algorithm, in which the fitting parameters were varied to minimize χ^2 between the measured and calculated reflectivity values. The fits of the reflectivity data were validated by constraining the surface excess $\gamma(z)$ within 20% of the dry sample thickness measured by ellipsometry. The surface excess was calculated using the following equation:

$$\gamma(z) = \int_0^\infty \phi(z)\mathrm{d}z \quad (5)$$

where $\phi(z)$ is the monomer volume fraction.

Results

The brush collapse was monitored by the change in the ellipsometric thickness Δd with respect to the initial swollen thickness $d_{sw}^{15\,°C}$ as a function of temperature, as shown in Fig. 1. The solid line represents the sigmoid function fitted to the experimental data, from which the transition temperature T_{tr} was extracted as the inflection point of the curve. As shown in Fig. 1a, the phase transition of the P(NIPAM-*b*-DMAEMA) brush is broader than for each single component, and it is extended over the entire range of PNIPAM and PDMAEMA collapse. The transition temperature T_{tr} considering the total phase transition is situated between that of the PNIPAM brush

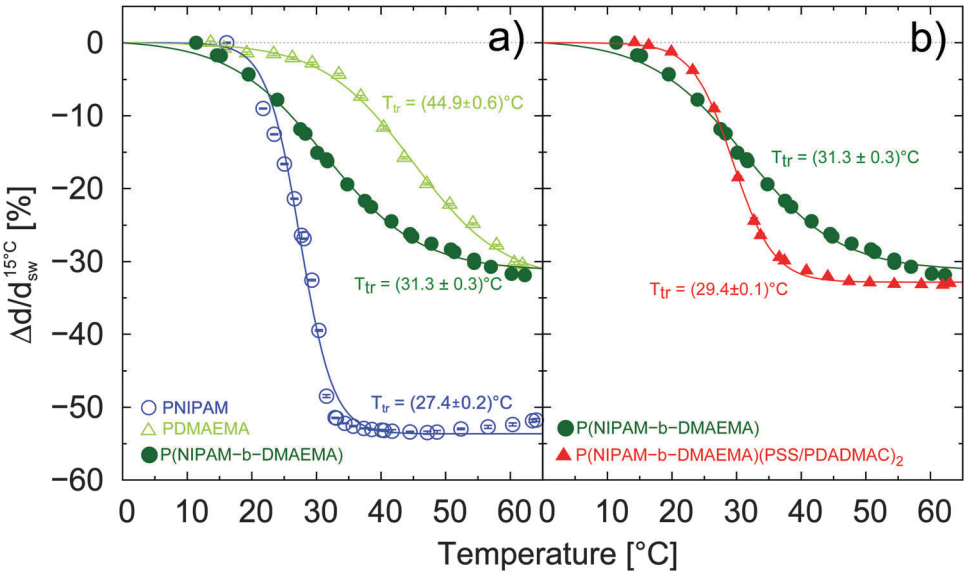

Fig. 1 Relative thickness change $\Delta d/d_{sw}^{15\,^{\circ}C}$, calculated according to eqn (3), as a function of heating temperature. In (a) the homopolymers PNIPAM and PDMAEMA are compared with the P(NIPAM-*b*-DMAEMA) brushes, while in (b) the block copolymer is compared with the P(NIPAM-*b*-DMAEMA)(PSS/PDADMAC)$_2$ system. The samples were swollen in Milli-Q water and the sample thickness was measured by ellipsometry. The solid lines represent the fit of a sigmoid function to the experimental data points. The transition temperature T_{tr} corresponds to the inflection point of the sigmoid. For the full symbols, the error bars are not visible as they are smaller than the symbols.

(~27 °C) and the PDMAEMA brush (~45 °C). Furthermore, the total degree of collapse is mostly dominated by the PDMAEMA block, where a lower collapse is achieved at (63 ± 1) °C compared to the pure PNIPAM brush. In fact, the partial charging of PDMAEMA (pK_a ~ 7.5[26]) in Milli-Q water (pH ~ 5.5) is likely to prevent the dehydration as strong as observed for the PNIPAM brush.

In Fig. 1b, the same collapse curve of the P(NIPAM-*b*-DMAEMA) brush is now compared with the corresponding (PSS/PDADMAC)$_2$-capped system. As mentioned above, the P(NIPAM-*b*-DMAEMA) brush showed a broad collapse over the entire range of investigated temperatures, whereas the composite system P(NIPAM-*b*-DMAEMA)(PSS/PDADMAC)$_2$ exhibited a steeper collapse, which occurred in a narrow temperature range between 20 and 35 °C. Besides this difference, the two systems reached a similar percentage of thickness decrease at high temperature (63 ± 1 °C), with little change in the T_{tr} when the collapse of the system as a whole is considered.

The ellipsometry data defined the average water content inside the entire polymer film, while the internal distribution of the monomer and water perpendicular to the substrate was revealed by neutron reflectometry. The reflectivity curves measured below (15 °C), across (35 °C) and above (65 °C) the phase transition are reported in Fig. 2a and b. From the fit on these data with a layer model, the corresponding SLD profiles were obtained and are reported in Fig. 2c and d. The fitting parameters are listed in Table S2 of the ESI.† For P(NIPAM-*b*-DMAEMA) at 15 °C (Fig. 2c), an extended region of the sample with constant SLD corresponds to the hydrated inner part of the polymer brush, likely PNIPAM and the initial part of the PDMAEMA block. The absence of contrast between the two polymers in the swollen state is not surprising, as they have similar SLD profiles and degrees of swelling. It follows a region of increasing SLD for the outermost part of the PDMAEMA block, which is characterized by an increasing degree of hydration (*i.e.* higher D_2O content), according to the enhanced ionization of the side groups towards the solution.[27,39]

When the temperature is increased to 35 °C, the system crosses the phase transition, as shown by the ellipsometry data in Fig. 1. In fact, evidence of dehydration close to the substrate is given by the decrease of the SLD, while high water content is maintained towards the brush/liquid interface. This indicates that at the phase transition temperature most of the hydration water is located in the PDMAEMA block, due to its higher hydrophilicity and therefore a higher phase transition temperature compared to the PNIPAM block (Fig. 1a). Finally, the dehydration of the entire brush is achieved at 65 °C, where the SLD drops further close to the substrate and the brush/D_2O interface becomes sharper.

For the brush/PEM system, similar changes in the SLD profiles for increasing temperature as observed for the brush were obtained. However, there are few important differences to be noticed. First of all, at 15 °C the PEM-capped system reaches a smaller degree of swelling compared to the pure brush, as shown in the SLD profile in Fig. 2c and d. Second, the region of constant SLD close to the solid substrate is thinner in the PEM-capped system (~300 Å), and the profile starts increasing to higher SLD. By heating up to 35 °C, a decrease of the SLD close to the substrate and at the region corresponding to the PDMAEMA/PEM interface is observed, ascribed to D_2O extrusion. Finally, at 65 °C the further shift of the SLD to lower values at the brush/substrate interface and the increased sharpness at the multilayer/D_2O interface indicate the full brush collapse and the dehydration of the PEM. It is noteworthy

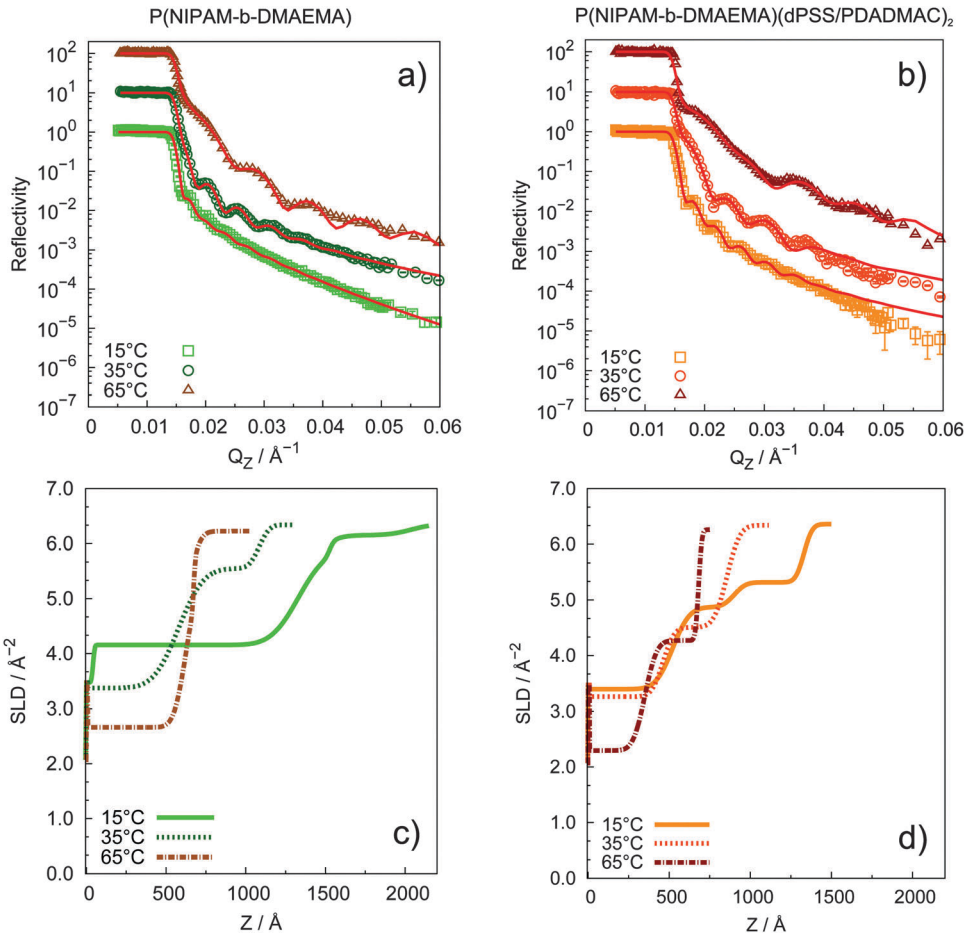

Fig. 2 (a and b) Neutron reflectivity curves measured below and above the phase transition temperature of the polymer brushes. The samples were swollen in deuterated water. The solid lines are the fits to the experimental data. The curves at 35 °C and 65 °C are offset by a scaling factor of 10 and 100, respectively, to ensure clarity. (c and d) Scattering length density (SLD) profiles obtained from the fit of the experimental data.

that also at high temperatures the region of constant SLD corresponding to the dehydrated brush is thinner than in the case of the pure block copolymer, and it increases continually to the value of the deuterated multilayer. Since at temperatures above the LCST the hydration water has been mostly expelled from the brush, the increasing SLD might be explained by the diffusion of deuterated PSS chains inside the PDMAEMA block during the dipping process and the complexation between the oppositely charged side groups of the two polymers. This aspect will be discussed in detail in the next section.

Discussion

The results reported in the previous section demonstrated the possibility of preparing brush/PEM composites by adsorbing polyelectrolyte multilayers onto a charged polymer-brush substrate, preserving its temperature-responsiveness. From the ellipsometry data reported in Table 1 it is possible to notice the much stronger thickness increase upon PEM adsorption (~49 nm) compared to the multilayer growth on the silicon substrate (~8 nm). Similar thickness increments were reported by Rühe and coworkers[22] for the adsorption of PMAA/MePVP (weak/strong PE pair) double layers onto PMAA brushes. Therein it was demonstrated that the PE adsorption increases with increasing thickness of the brush substrate and with the use of weak polyelectrolytes, which form more soluble, and therefore more swollen, PE pairs and allow higher mass uptake. Their findings explain the high thickness increment observed for a 2-double-layer PEM adsorbed onto PDMAEMA brushes (Table 1). Interestingly, despite the strong thickness difference under ambient conditions, P(NIPAM-*b*-DMAEMA) and the $(PSS/PDADMAC)_2$-capped system have similar degrees of swelling (Fig. 2c, d and Table 1). This might be explained by the complexation between PSS chains and the PDMAEMA block, which reduces its partial charging and hydrophilicity. This hypothesis is supported by the change in temperature-responsive behavior of P(NIPAM-*b*-DMAEMA) brushes upon PEM adsorption. The relative change in the ellipsometric thickness at increasing temperature (Fig. 1) highlighted the interesting aspects of the temperature responsive behavior of both P(NIPAM-*b*-DMAEMA) and the $(PSS/PDADMAC)_2$-capped system. First of all, in contrast to previous findings on statistic copolymers of PNIPAM and alkylacrylic acids (aAAs),[40] the temperature responsive behavior of P(NIPAM-*b*-DMAEMA)

is preserved and it results from the individual contribution of each polymer block. The significant difference between P(NIPAM-*b*-DMAEMA) brushes and the corresponding (PSS/PDADMAC)$_2$-capped system, with the smooth collapse over a broad temperature range for the block copolymer and a steeper phase transition for the brush/PEM system, can be explained by an enhanced hydrophobization of the PDMAEMA block. It is likely that during the dipping of the brush substrate into the negatively charged PSS solution some chains diffuse into the brush and form complexes with the oppositely charged PDMAEMA side groups, leading to a partial charge compensation of PDMAEMA by PSS. This reduces the charge density of the weak polyelectrolyte block and connects the adjacent PDMAEMA chains, with the result of shifting its phase transition to lower temperatures. This in turn causes the overlapping of PDMAEMA collapse with the PNIPAM one. The hypothesis of diffusion and accumulation of PSS chains inside the brush is supported by the SLD profile of the brush/multilayer system reported in Fig. 2d: at small distances and at any temperature, *i.e.* also when D_2O extrusion occurred at a high temperature (65 °C), the SLD increases to higher values in the region corresponding to the PDMAEMA brush. The shift of phase transition temperature to lower values due to hydrophobization effects has been discussed in the literature.[41–43] In general, the enhanced hydrophobicity may arise from reduced charged density[41] (*e.g.* by the change in pH), the presence of more hydrophobic side groups,[42] or the combination with more hydrophobic comonomers.[43] Moreover, a higher rate of collapse for more hydrophobic poly(methacrylates) has also been discussed by Wanless and coworkers,[44] whose findings would be in agreement with the narrower collapse of the brush/PEM composite observed in Fig. 1b. It might be argued that the plateau reached by P(NIPAM-*b*-DMAEMA)(PSS/PDADMAC)$_2$ around 40 °C might indicate the absence of PDMAEMA collapse due to the steric hindrance exerted by PSS chains. In that case a reduced degree of collapse would be expected, which is not observed in Fig. 1b, where the two systems reach the same degree of collapse. Therefore this hypothesis is excluded here.

The monomer distribution at different temperatures revealed by NR is in good agreement with the collapse profiles obtained by ellipsometry. In the case of P(NIPAM-*b*-DMAEMA) brushes, the stepwise decrease of the SLD due to D_2O extrusion at increasing temperatures is consistent with the smooth brush collapse observed in Fig. 1.

The SLD profiles reported in Fig. 2c are in good agreement with the behavior of the subsystems, PNIPAM and the PDMAEMA brush, reported by previous neutron reflectometry studies.[28,45] In particular, for PNIPAM brushes with comparable grafting density and thickness as those presented in this work,[45] a broad monomer distribution perpendicular to the substrate was found at 20 °C, which was described by a bilayer profile, in contrast to the more uniform, steplike profile at 41 °C. Surface plasmon resonance experiments confirmed such a structural picture, with a region close to the substrate continuously dehydrating between 10 and 40 °C, and an outermost part which remained highly solvated until the transition temperature (about 32 °C) is reached.[46] Titmuss and coworkers[28] observed a similar behavior for the PDMAEMA brush swollen at pH = 10 across the phase transition. A partial collapse with a more significant dehydration close to the substrate was found between 30 and 40 °C, leading to a bilayer structure with a denser inner part and a dilute outer region. Further dehydration was measured between 40 and 50 °C. These features can also be recognized in the temperature dependent collapse of the P(NIPAM-*b*-DMAEMA) copolymer reported in Fig. 2c in the first phase transition between 15 to 35 °C, the PNIPAM brush collapses mostly in the region close to the substrate, with the more hydrated outer part extending to the swollen PDMAEMA; in the second step between 35 and 65 °C also the PDMAEMA brush collapses leading to a sharp brush/liquid interface. This description of the phase transition of the P(NIPAM-*b*-DMAEMA) brush supports the ellipsometry curves in Fig. 1 showing the individual contribution of each polymer block.

In the case of the P(NIPAM-*b*-DMAEMA)(dPSS/PDADMAC)$_2$ system, the strong contraction at the PEM/liquid interface observed in the SLD profile corresponds to the sharp thickness decrease between 15 and 35 °C. Moreover, for this system the presence of deuterated PSS chains inside the hydrogenated brushes is validated by the increasing SLD values at small distances from the substrate, likely the PNIPAM block, towards the outermost PEM. The inflection points of the SLD profile at 65 °C (Fig. 2c and d), which are considered the reference positions for the interface between hydrogenated and deuterated media, are located at about 600 Å for P(NIPAM-*b*-DMAEMA), and at ~300 Å and ~600 Å for the corresponding PEM-capped system. While the outermost interface corresponds to the film/D_2O region in both cases, the inner interface of the brush/multilayer composite is likely located between PNIPAM and the PDMAEMA block, whose enhanced contrast is due to the diffusion of dPSS inside the entire polyelectrolyte brush.

Conclusion

The studies carried out on the temperature responsive behavior of P(NIPAM-*b*-DMAEMA) brushes and the corresponding (PSS/PDADMAC)$_2$-capped system demonstrated that it is possible to combine brush and multilayer blocks without compromising their responsive character. Some important effects arising from the interaction between the two systems were found. In particular, the ellipsometry studies showed that the smooth thickness decrease of P(NIPAM-*b*-DMAEMA) brushes, which is the result of a continuous phase transition from the contribution of both PNIPAM and PDMAEMA, became a steeper collapse for the multilayer-capped system. This behavior was explained by the enhanced hydrophobization of the PDMAEMA block by charge compensation with PSS chains, diffusing into the brush during the polyelectrolyte adsorption. The reduced charge density of PDMAEMA was responsible for the decreased phase transition temperature, causing the overlapping of the PDMAEMA collapse with the PNIPAM one. The suppression of PDMAEMA collapse by the PSS/PDMAEMA interaction was excluded, because the percentage of collapse reached by the brush/PEM system was similar to the one measured for the pure brush.

The diffusion of PSS chains into the charged region of the block copolymer was proved by comparing the SLD profiles obtained by NR measurements on both systems under investigation. Only a region of about 30 nm with constant SLD was found in the vicinity of the solid substrate for the P(NIPAM-*b*-DMAEMA)(dPSS/PDADMAC)$_2$ system, corresponding to the PNIPAM brush. The region with increasing SLD was ascribed to the PDMAEMA/dPSS, proving the diffusion of dPSS inside the PDMAEMA block.

The presence of PEMs also had an influence on the collapse behavior of the brush: first of all, the D_2O uptake of the brush was reduced in the proximity of the solid substrate; secondly, while for the pure brush a stepwise dehydration at the brush/silicon substrate was observed for increasing temperature, the dehydration of the PEM-capped system caused a significant contraction at the PDMAEMA/PEM region between 15 and 35 °C, supporting the hypothesis of the occurrence of PDMAEMA phase transition in this range of temperature.

It is worth mentioning that a large number of parameters influence the uptake of polymers and their interaction with the brush matrix. Therefore any change in the monomer functionality and the environment (solvent, pH, ionic strength) has a significant influence on the adsorbed amount, the distribution inside the matrix, the strength and nature of interaction and the switching behavior of the polymer brush upon applied stimuli. At the same time, such a large variety of effects are the key for the creation of a broad array of multicompartment systems, which constitute more sophisticated, but also more adequate and on-demand smart coatings.

Acknowledgements

The authors S. M. and R. v. K. are grateful to the International Graduate School IRTG 1524 (DFG) for financial support. The Heinz Maier-Leibnitz Zentrum is acknowledged for the beamtime allocated at the neutron reflectometer NREX. The polymer PDADMAC was a kind gift from André Laschwesky (Fraunhofer Institute of Applied Polymer Research IAP and University of Potsdam).

References

1 R. Barbey, L. Lavanant, D. Paripovic, N. Schüwer, C. Sugnaux, S. Tugulu and H.-A. Klok, Polymer brushes *via* surface-initiated controlled radical polymerization: synthesis, characterization, properties, and applications, *Chem. Rev.*, 2009, **109**, 5437–5527.

2 P. Lavalle, J. C. Voegel, D. Vautier, B. Senger, P. Schaaf and V. Ball, Dynamic aspects of films prepared by a sequential deposition of species: perspectives for smart and responsive materials, *Adv. Mater.*, 2011, **23**, 1191–1221.

3 R. von Klitzing, Internal structure of polyelectrolyte multilayer assemblies, *Phys. Chem. Chem. Phys.*, 2006, **8**, 5012–5033.

4 R. Toomey and M. Tirrell, Functional polymer brushes in aqueous media from self-assembled and surface-initiated polymers, *Annu. Rev. Phys. Chem.*, 2008, **59**, 493–517.

5 A. Olivier, F. Meyer, J.-M. Raquez, P. Damman and P. Dubois, Surface-initiated controlled polymerization as a convenient method for designing functional polymer brushes: From self-assembled monolayers to patterned surfaces, *Prog. Polym. Sci.*, 2012, **37**, 157–181.

6 M. P. Weir and A. J. Parnell, Water Soluble Responsive Polymer Brushes, *Polymers*, 2011, **3**, 2107–2132.

7 X. Zhang, P. Yang, Y. Dai, P. Ma, X. Li, Z. Cheng, Z. Hou, X. Kang, C. Li and J. Lin, Multifunctional Up-Converting Nanocomposites with Smart Polymer Brushes Gated Mesopores for Cell Imaging and Thermo/pH Dual-Responsive Drug Controlled Release, *Adv. Funct. Mater.*, 2013, **23**, 4067–4078.

8 P. Akcora, H. Liu, S. K. Kumar, J. Moll, Y. Li, B. C. Benicewicz, L. S. Schadler, D. Acehan, A. Z. Panagiotopoulos, V. Pryamitsyn, V. Ganesan, J. Ilavsky, P. Thiyagarajan, R. H. Colby and J. F. Douglas, Anisotropic self-assembly of spherical polymer-grafted nanoparticles, *Nat. Mater.*, 2009, **8**, 354–359.

9 J. B. Bünsow, T. I. M. S. Kelby and W. T. S. Huck, Polymer Brushes: Routes toward Mechanosensitive Surfaces, *Acc. Chem. Res.*, 2010, **43**, 466–474.

10 C.-J. Huang, Y.-S. Chen and Y. Chang, Counterion-Activated Nanoactuator: Reversibly Switchable Killing/Releasing Bacteria on Polycation Brushes, *ACS Appl. Mater. Interfaces*, 2015, **7**, 2415–2423.

11 M. Kobayashi, Y. Terayama, H. Yamaguchi, M. Terada, D. Murakami, K. Ishihara and A. Takahara, Wettability and antifouling behavior on the surfaces of superhydrophilic polymer brushes, *Langmuir*, 2012, **28**, 7212–7222.

12 K. Glinel, A. M. Jonas, T. Jouenne, J. Leprince, L. Galas and W. T. S. Huck, Antibacterial and antifouling polymer brushes incorporating antimicrobial peptide, *Bioconjugate Chem.*, 2009, **20**, 71–77.

13 A. Naderi, R. Makuška and P. M. Claesson, Interactions between bottle-brush polyelectrolyte layers: effects of ionic strength and oppositely charged surfactant, *J. Colloid Interface Sci.*, 2008, **323**, 191–202.

14 P. M. Claesson, R. Makuska, I. Varga, R. Meszaros, S. Titmuss, P. Linse, J. S. Pedersen and C. Stubenrauch, Bottle-brush polymers: Adsorption at surfaces and interactions with surfactants, *Adv. Colloid Interface Sci.*, 2010, **155**, 50–57.

15 G. Sudre, L. Olanier, Y. Tran, D. Hourdet and C. Creton, Reversible adhesion between a hydrogel and a polymer brush, *Soft Matter*, 2012, **8**, 8184–8193.

16 G. Sudre, D. Hourdet, C. Creton, F. Cousin and Y. Tran, Probing pH-Responsive Interactions between Polymer Brushes and Hydrogels by Neutron Reflectivity, *Langmuir*, 2014, **30**, 9700–9706.

17 S. Gupta, M. Agrawal, P. Uhlmann, F. Simon, U. Oertel and M. Stamm, Gold nanoparticles immobilized on stimuli responsive polymer brushes as nanosensors, *Macromolecules*, 2008, **41**, 8152–8158.

18 S. Christau, S. Thurandt, Z. Yenice and R. von Klitzing, Stimuli-Responsive Polyelectrolyte Brushes As a Matrix for the Attachment of Gold Nanoparticles: The Effect of Brush Thickness on Particle Distribution, *Polymers*, 2014, **6**, 1877–1896.

19 S. Christau, T. Möller, Z. Yenice, J. Genzer and R. von Klitzing, Brush/gold nanoparticle hybrids: Effect of grafting density on particle uptake and distribution within weak polyelectrolyte brushes, *Langmuir*, 2014, **30**, 13033–13041.
20 J. Shan, J. Chen, M. Nuopponen and H. Tenhu, Two Phase Transitions of Poly(*N*-isopropylacrylamide) Brushes Bound to Gold Nanoparticles, *Langmuir*, 2004, **20**, 4671–4676.
21 H. Zhang and J. Rühe, Interaction of strong polyelectrolytes with surface-attached polyelectrolyte brushes-polymer brushes as substrates for the layer-by-layer deposition of polyelectrolytes, *Macromolecules*, 2003, **36**, 6593–6598.
22 H. Zhang and J. Rühe, Weak Polyelectrolyte Brushes as Substrates for the Formation of Surface-Attached Polyelectrolyte-Polyelectrolyte Complexes and Polyelectrolyte Multilayers, *Macromolecules*, 2005, **38**, 10743–10749.
23 P. Laurent, G. Souharce, J. Duchet-Rumeau, D. Portinha and A. Charlot, 'Pancake' *vs.* brush-like regime of quaternizable polymer grafts: an efficient tool for nano-templating polyelectrolyte self-assembly, *Soft Matter*, 2012, **8**, 715–725.
24 S. E. Moya, J. J. Iturri Ramos and I. Llarena, Templation, water content, and zeta potential of polyelectrolyte nano-assemblies: a comparison between polyelectrolyte multilayers and brushes, *Macromol. Rapid Commun.*, 2012, **33**, 1022–1035.
25 E. Wischerhoff, S. Glatzel, K. Uhlig, A. Lankenau, J.-F. Lutz and A. Laschewsky, Tuning the thickness of polymer brushes grafted from nonlinearly growing multilayer assemblies, *Langmuir*, 2009, **25**, 5949–5956.
26 P. V. D. Wetering, E. E. Moret, N. M. E. Schuurmans-Nieuwenbroek, M. J. V. Steenbergen and W. E. Hennink, Structure-Activity Relationships of Water-Soluble Cationic Methacrylate/Methacrylamide Polymers for Nonviral Gene Delivery, *Bioconjugate Chem.*, 1999, **10**, 589–597.
27 M. Moglianetti, J. R. P. Webster, S. Edmondson, S. P. Armes and S. Titmuss, Neutron reflectivity study of the structure of pH-responsive polymer brushes grown from a macro-initiator at the sapphire-water interface, *Langmuir*, 2010, **26**, 12684–12689.
28 H. Jia, A. Wildes and S. Titmuss, Structure of pH-Responsive Polymer Brushes Grown at the Gold–Water Interface: Dependence on Grafting Density and Temperature, *Macromolecules*, 2012, **45**, 305–312.
29 H. Dautzenberg, E. Görnitz and W. Jaeger, Synthesis and characterization of poly(diallyldimethylammonium chloride) in a broad range of molecular weight, *Macromol. Chem. Phys.*, 1998, **199**, 1561–1571.
30 T. Fujie, J. Y. Park, A. Murata, N. C. Estillore, M. C. R. Tria, S. Takeoka and R. C. Advincula, *Appl. Mater. Interfaces*, 2009, **1**, 1404–1413.
31 E. D. Bain, K. Dawes, A. O. Evren, X. Hu, C. B. Gorman, S. Jir and J. Genzer, Surface-Initiated Polymerization by Means of Novel, Stable, Non-Ester-Based Radical Initiator, *Macromolecules*, 2012, **45**, 3802–3815.
32 G. Decher, Fuzzy Nanoassemblies: Toward Layered Polymeric Multicomposites, *Science*, 1997, **277**, 1232–1237.
33 J. B. Theeten and D. E. Aspnes, Ellipsometry in Thin Film Analysis, *Annu. Rev. Mater. Sci.*, 1981, **11**, 97–122.
34 H. G. Tompkins, *Handbook of Ellipsometry*, 2005, vol. 30, pp. 92–94.
35 M. Zerball, A. Laschewsky and R. von Klitzing, Swelling of Polyelectrolyte Multilayers: The Relation between Surface and Bulk Characteristics, *J. Phys. Chem. B*, 2015, **119**, 11879–11886.
36 J. R. Howse, E. Manzanares-Papayanopoulos, I. a. McLure, J. Bowers, R. Steitz and G. H. Findenegg, Critical adsorption and boundary layer structure of 2-butoxyethanol + D_2O mixtures at a hydrophilic silica surface, *J. Chem. Phys.*, 2002, **116**, 7177–7188.
37 S. Dodoo, R. Steitz, A. Laschewsky and R. von Klitzing, Effect of ionic strength and type of ions on the structure of water swollen polyelectrolyte multilayers, *Phys. Chem. Chem. Phys.*, 2011, **13**, 10318–10325.
38 A. Nelson, Co-refinement of multiple-contrast neutron/X-ray reflectivity data using MOTOFIT, *J. Appl. Crystallogr.*, 2006, **39**, 273–276.
39 S. Sanjuan, P. Perrin, N. Pantoustier and Y. Tran, Synthesis and swelling behavior of pH-responsive polybase brushes, *Langmuir*, 2007, **23**, 5769–5778.
40 Y. Lu, A. Zhuk, L. Xu, X. Liang, E. Kharlampieva and S. a. Sukhishvili, Tunable pH and temperature response of weak polyelectrolyte brushes: role of hydrogen bonding and monomer hydrophobicity, *Soft Matter*, 2013, **9**, 5464–5472.
41 T. G. Park and A. S. Hoffman, Synthesis and characterization of pH- and/or temperature-sensitive hydrogels, *J. Appl. Polym. Sci.*, 1992, **46**, 659–671.
42 T. Thavanesan, C. Herbert and F. a. Plamper, Insight in the phase separation peculiarities of poly(dialkylaminoethyl methacrylate)s, *Langmuir*, 2014, **30**, 5609–5619.
43 M. Nakayama and T. Okano, Polymer terminal group effects on properties of thermoresponsive polymeric micelles with controlled outer-shell chain lengths, *Biomacromolecules*, 2005, **6**, 2320–2327.
44 J. D. Willott, B. a. Humphreys, T. J. Murdoch, S. Edmondson, G. B. Webber and E. J. Wanless, Hydrophobic effects within the dynamic pH-response of polybasic tertiary amine methacrylate brushes, *Phys. Chem. Chem. Phys.*, 2015, **17**, 3880–3890.
45 H. Yim, M. S. Kent, S. Satija, S. Mendez, S. S. Balamurugan, S. Balamurugan and G. P. Lopez, Study of the conformational change of poly(*N*-isopropylacrylamide)-grafted chains in water with neutron reflection: Molecular weight dependence at high grafting density, *J. Polym. Sci., Part B: Polym. Phys.*, 2004, **42**, 3302–3310.
46 S. Balamurugan, S. Mendez, S. S. Balamurugan, M. J. O'Brie and G. P. López, Thermal Response of Poly(*N*-isopropylacrylamide) Brushes Probed by Surface Plasmon Resonance, *Langmuir*, 2003, **19**, 2545–2549.